A Hybrid Time-Efficient Modeling Approach for Acoustic Noise Prediction in SRMs

Ziyan Zhang, Zichao Jin, Chengxiu Chen, Selin Yaman, Mahesh Krishnamurthy
Electric Drives and Energy Conversion Laboratory
Illinois Institute of Technology, Chicago, IL 60616 USA
EML: kmahesh@iit.edu; URL: http://drives.ece.iit.edu

Abstract- This study presents a computationally cost-effective modeling approach for a switched reluctance machine (SRM) towards predicting vibration and acoustic noise. In the proposed approach, the SRM is modeled using Finite Element (FE) software for capturing magnetic snapshots from static simulations. Using an advanced field reconstruction method (FRM), these snapshots are used to develop basis functions to estimate magnetic fields under any arbitrary stator excitation and at any desired rotor position. This method includes magnetic properties of the machine and can estimate flux density at once instead of partially predicting it. The vibration model is built in FE software while the acoustic noise is predicted using the analytical method. The proposed study can significantly reduce the computational time for vibration and noise analysis with decent accuracy. Dynamic simulation by finite-element analysis (FEA) software and experimental verification have been carried out to verify the effectiveness of the proposed hybrid model.

I. INTRODUCTION

Acoustic and vibration issues are crucial to the switched reluctance machine design process. The sources of acoustic noise and vibration of SRM could be magnetic, mechanical, and electrical [1]. Researchers have shown that the radial force that produced by the magnetic flux in air gap can cause the vibration of excited stator and rotor, hence it becomes the main source of acoustic noise [2]. To analyze and predict the noise generated by the electromagnetic forces, it is necessary to build mathematical models including motor electromagnetic model, structural vibration model and structure acoustic response model. The finite element method (FEM) is the most well known method for motor numerical analysis and multi-physics problems. The boundary element method (BEM) is also a popular approach and widely used to calculate the noise radiation into a space [3-4].

For the electromagnetic model, the electromagnetic force can be calculated by Maxwell Stress Tensor method, the Equivalent Magnetic Sources methods, the Virtual Work principle approaches, and eggshell method [5-10]. The Maxwell Stress tensor method is easy to implement and it costs less in terms of computation cost with fair accuracy. Both the accuracy and computation cost of the equivalent magnetic source based methods are worse than Maxwell Stress tensor method. Therefore, it is rarely used in vibration analysis of electric machine. Although the Virtual Work Principle methods are most accurate and versatile, it needs much more computation resources. The eggshell approach is equivalent to the Maxwell Stress tensor and the Virtual Work Principle

methods. Researches had shown that it has several advantages compared to other methods in practices and principles [10-12]. Furthermore, it has been used for magnetic force analysis in electric machine and actuator which shows potential of this method [13-15].

With the electromagnetic force calculated from electromagnetic model, the structural vibration model can be built to represent the deformation and oscillations of motor. Usually, the modal analysis and harmonic forced response analysis are done for stator vibration study. The rotor vibration is neglected in most cases since its natural frequency is quite high. The natural frequency or eigenvalue and the corresponding undamped free vibration modes can be obtained by assuming no applied force by modal analysis. Harmonic response analysis computes the amplitude of response of a structure to a set of loads which is originated from the electromagnetic force for electric machines. There are a few methods that are utilized for the modal analysis and harmonic response analysis, which include direct integration method, reduced method, and modal superposition method. The direct integration method does not need special transformation, which makes it simple to be implemented with relatively good accuracy, but requires longer solution time [16-19]. Both reduced methods and modal superposition method can reduce the order of the FE model and save the solution time. The modal superposition method is faster, but it cannot be applied for nonlinear material [19-22].

The FEM method has been well established for calculating the acoustic fields. The objective equations can be solved efficiently and accurately. However, it is only suitable for interior sound field or near sound field acoustic radiation problems. For far field acoustic radiation studies, infinite acoustic radiation could be an issue. The entire volume close to infinity must be discretized, which requires very large amount of data to calculate the sound radiation [23-25]. The BEM method is more applicable for sound propagation problems, where only the surface of area needs to be discretized [3-4].

Compared with the numerical methods, the analytical method is much easier to be implemented and greatly saves the computational time. Therefore, in this paper, a semi-analytical acoustic model has been developed and verifies on a 6/10 HRSRM. By using the magnetic snapshots from 2D FEA model, an improved FRM method was implemented to build the basis function and estimate the flux density in the

electromagnetic model, in the mean time, the Maxwell Stress Tensor method was used for radial force calculation. The mode frequencies were obtained from FEA software from the structural model and sound pressure level of the SRM was calculated by analytical expressions. The modeling process is shown in the flow chart in Fig.1. The estimation results of the proposed model were compared with with FEA model results and experimental results.

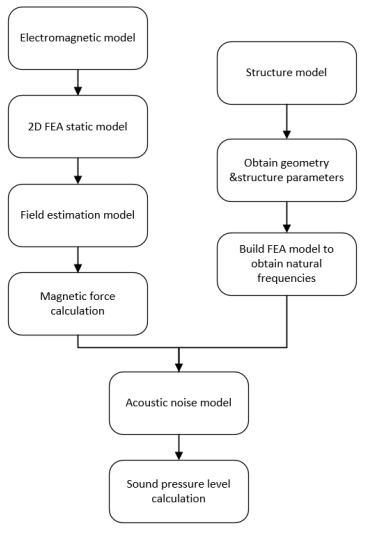


Fig. 1. Flowchart of time efficient acoustic noise estimation model

II. ELECTROMEGANETIC MODEL

The electromagnetic model is developed for field estimation in order to develop the relationship between excitation current and flux density. The SRM is modeled using a 2D FEA model to calculate the flux density components in both radial and tangential directions along the circular contour defined in the middle of the airgap. Next, the data fitting method is used to get the full cycle inductance profile from the magnetic snapshots. Using this information, the basis functions are created, which are crucial in predicting the magnetic fields for any stator excitation and at any position on a circular contour of the middle of airgap. Traditionally, basis functions are developed using FRM since it is an effective method for torque ripple minimization and calculation of vibration. The details of this method and application are given in [26-27]. The computation of FRM uses a truncated Fourier series expansion, which is used for each point on the contour. The calculation can be complicated and time consuming. Also, the accuracy is closely related to the number of contour points and FEA magnetic field solutions. This section presents an advanced FRM that can greatly reduce the computational time with a decent accuracy. After obtaining flux density from the improved FRM, the electromagnetic forces can be calculated by Maxwell Stress Tensor method.

A. Data fitting

In order to reflect the dependency upon rotor position, a position estimation agent is needed. Since the SRM is

inherently doubly salient, it is necessary to use a fitting estimation method for position estimations. Gaussian fit, Sum of sine fit, and Polynomial fit are three basic data fitting methods. The analytical expressions of these methods are shown in Table I.

TABLE I
TYPE SIZES FOR CAMERA-READY PAPERS ANALYTICAL EXPRESSIONS OF
ESTIMATION METHODS

| Method | Expression |
|-----------------|---|
| Gaussian fit | $f(x) = \sum_{k}^{N} a_k e^{-\left(\frac{x - b_k}{c_k}\right)^2}$ |
| Polynomial fit | $f(x) = \sum_{k}^{N} p_k x^N$ |
| Sum of sine fit | $f(x) = \sum_{k=0}^{N} a_k \sin(b_k x + c_k)$ |

The curve fitting results of the inductance profile with the three methods are shown in Fig. 2 to Fig. 4, respectively. Based on the analysis, the sum of sine approach has the best performance for matching the inductance profile at both saturated and unsturated region compare with the other two methods. Therefore, it is applied in the electromagnetic model.

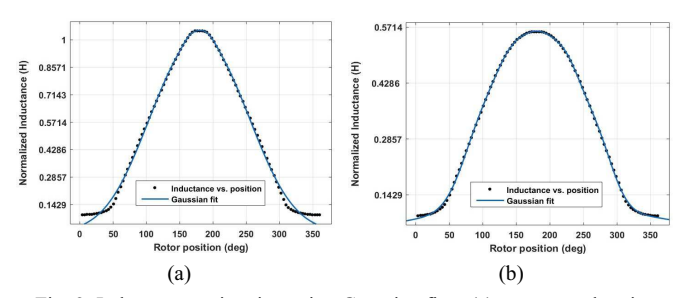


Fig. 2. Inductance estimation using Gaussian fit at (a) unsaturated region

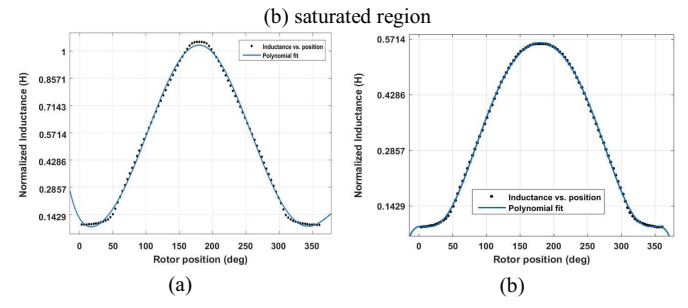


Fig. 3. Inductance estimation using Polynomial fit at (a) unsaturated

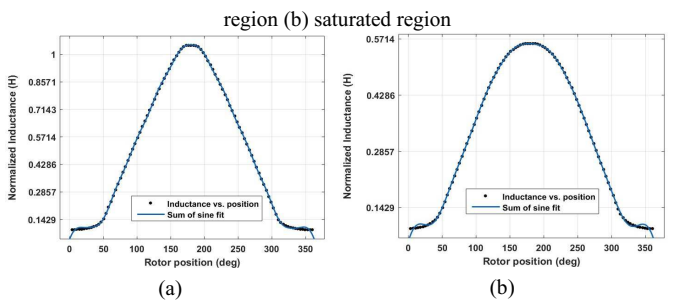


Fig. 4. Inductance estimation using Sum of sine fit at (a) unsaturated region (b) saturated region

A. Field Reconstruction Method

After obtaining the expression for inductance, the advanced FRM is implemented to the electromagnetic model to estimate the flux density. The basis functions is developed to present the relationship of flux density with the excitation current and rotor position, which can be expressed as follows for both radial and tangential directions,

$$B(i, \theta_r) = i \cdot T(i, \theta_r) \tag{1}$$

$$T(i, \theta_r) = P \cdot D(i) \tag{2}$$

where i is the excitation current, θ_r is the rotor position angle, $B(i, \theta_r)$ is the flux density components at radial (B_R) or tangential direction (B_T) , $T(i, \theta_r)$ is the estimation factor is defined by rotor position and excitation current. P is the position matrix that represents the rotor position dependency of SRM. It is derived based on the previous analysis as given in (3).

$$P = \begin{bmatrix} 1 & \cdots & 1 \\ a_1 \sin(b_1 \theta_{r_1} + c_1) & \cdots & a_1 \sin(b_1 \theta_{r_{2N}} + c_1) \\ \vdots & \ddots & \vdots \\ a_1 \sin(b_N \theta_{r_1} + c_N) & \cdots & a_1 \sin(b_N \theta_{r_{2N}} + c_N) \end{bmatrix}^{-1}$$
(3)

When determining the coefficients of position matrix, the nonlinearities of the SRM should be considered. A multiplier is introduced to represent the B–H characteristics of the core materials. This multiplier is conditioned by the rows of corresponding coefficients of excitation current where q is the number of current samples.

$$D(i) = \begin{bmatrix} d_1(i) & 0 & 0 & \cdots & 0 \\ 0 & d_2(i) & 0 & \cdots & 0 \\ 0 & 0 & d_3(i) & \cdots & 0 \\ \vdots & \vdots & \vdots & \ddots & \vdots \\ 0 & 0 & 0 & \cdots & d_{2N+4}(i) \end{bmatrix}$$
(4)

$$d_q(i) = \sum_{q=0}^{q_max} \frac{B_q(i)}{i_q}$$
 (5)

The least square fitting method is used for calculating the coefficients given by (6), where given input data x_{data} , and the observed output y_{data} , x_{data} and y_{data} are matrices or vectors, and $f(x, x_{data})$ is a matrix-valued or vector-valued function of the same size as y_{data} .

$$\min_{x} \|f(x, x_{data}) - y_{data}\|_{2}^{2} = \min_{x} \sum_{x} ((x, x_{data_{i}}) - y_{data_{i}})^{2}$$
 (6)

In this estimation, x_{data} and y_{data} are current and airgap flux profile, respectively. With the position matrix and estimation factor, the flux density with respect to any current and rotor position can be obtained by equation (1).

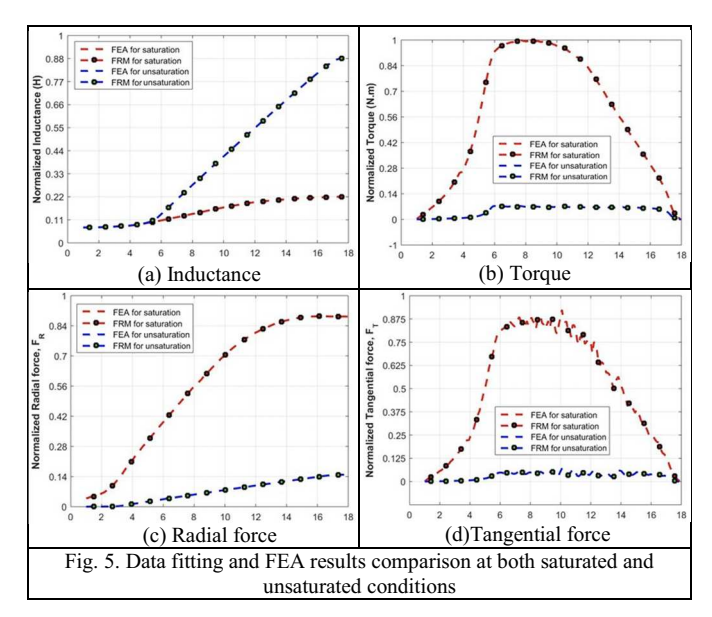
C. Radial force

The Maxwell Stress Tensor method is implemented to calculate the force density on the contour in the middle of the airgap due to its simplicity and decent accuracy. The tangential force (F_T) and radial (F_R) force are presented in (7) and (8), respectively, where μ_0 is the permeability of air.

$$F_T = \frac{B_R(i, \theta_r)B_T(i, \theta_r)}{\mu_0} \tag{7}$$

$$F_{R} = \frac{B_{R}^{2}(i, \theta_{r}) - B_{T}^{2}(i, \theta_{r})}{2\mu_{0}}$$
 (8)

The data fitting results are presented in Fig. 5 and compared to FEA results for both saturation and unsaturated condition. The simulation model is built based on a SRM with six stator poles and ten rotor poles. As the figures shows, the curve fitting of inductance, torque, and the electromagnetic forces match perfectly with the FEA simulation results.



III. STRUCTURAL MODEL

The vibration of SRM reaches the maximum value and generates excessive noise when the harmonics of radial force meet the natural frequency and cause resonance [28]. Thus, mode shapes and resonant frequencies of the stator system are important in the vibration analysis of electric machines. Most written literature [29-31] define the resonance frequency of the stator system at the circumferential vibrational mode m as:

$$f_m = \frac{1}{2\pi} \sqrt{\frac{K_m}{M_m}} \tag{9}$$

where K_m is the lumped stiffness and M_m is the lumped mass of the stator system. Most of the analytical methods consider the stator system as the cylindercal cell, some of them include the geometries of winding and frame, the end bells and foot mount can only be represented as a coefficient. None of the

analytical method have been found that include the modeling of fixed support and fins. So, the analytical method can not model the realistic condition of machine accurately. Therefore, the FEA model is built in ANSYS for obtaining the vibration modes and natural frequencies in this study.

The magnetic flux across the air gap produces radial force which excites several mode shapes. Each mode shape has its own natural frequency, which is determined by the geometry and material of electric machine. From a vibration perspective, modal analysis identifies the critical modes such that during the operation it could avoid triggering the resonance modes of the machine. This necessity sources from having significantly high vibration and acoustic peaks specifically on natural frequencies of the body. Fig. 6 shows the experimental validation for the mode shapes of Mode 2 that obtained from FEA simulation. The windings and isolation material in FEA model has been set to invisible in order to observe the deformation of the stator. Fig. 7 presents resonant frequencies for more modes.

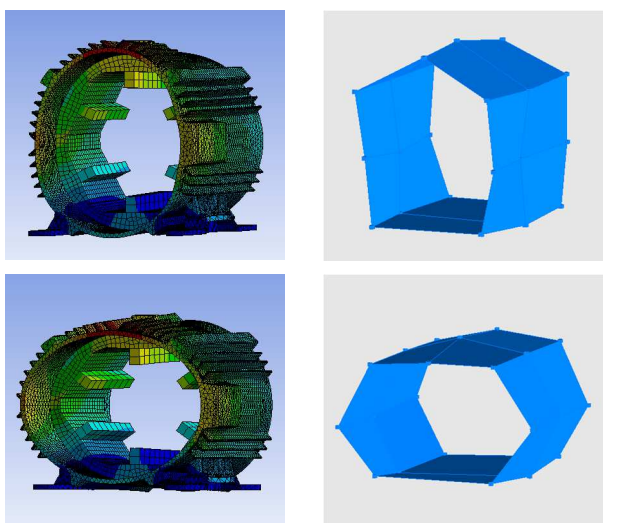


Fig. 6. Mode shapes from FEA simulation and experimental test (Mode 2)

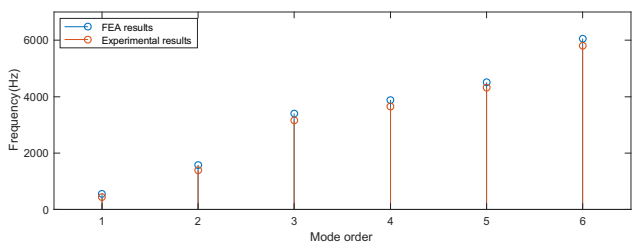


Fig. 7. Natural frequencies comparison of FEA and experimental results

These mode shapes are titled under radial vibration. Stator teeth deflect in the tangential direction, which implies that tangential electromagnetic force has effect on tangential deformation in high frequency range. Also, force excitation in high frequency is not always the same on every tip. Hence, the

interaction between tips makes mode shapes irregular, however, the deflection value is quite small.

Damping ratio is one of the main components to analyze the stator vibration. The amplitudes of stator vibration decay are determined by the damping ratio. Empirical expression for mechanical damping of the stator for the small and medium sized electrical machines is suggested as in the expression given below, where ξ_m is model damping ratio, f_m is the natural frequency [29].

$$\xi_m = \frac{1}{2\pi} (2.76 \times 10^{-5} f_m + 0.062) \tag{10}$$

IV. ACOUSTIC NOISE PREDICTION

For proper estimation of audible noise, determination of excitation frequencies is critical. Excitation frequency is calculated based on the following equation, where $n = 1,2,3..., \omega$ is the speed of the machine and N_r is the number of rotor poles.

$$f_n = \frac{nN_r\omega}{60} \tag{11}$$

With the radial force from electromagnetic model and natural frequencies from structure model, acoustic noise level can be calculated. The first step is to calculate the radiated sound power from the outer surface of the stator for mode 'm' by using the following equation [32],

$$\Pi_m = \rho_0 c_0 S_h (\frac{\omega A_m}{\sqrt{2}})^2 \sigma_m \tag{12}$$

where ρ_0 and c_0 are the density and sound speed in the ambient air, respectively, S_h is the outer surface of the housing which given by

$$S_h = \pi D_h L_h \tag{13}$$

where D_h is the outer diameter of the housing, L_h is length of housing, ω is the rotation speed of motor, and A_m is the radial vibration displacement given by,

$$A_{m} = \frac{F_{r,f_{n}}/M}{\sqrt{(\omega_{m}^{2} - w_{n}^{2})^{2} + 4\xi_{m}^{2}\omega_{m}^{2}\omega_{n}^{2}}}$$
(14)

where F_{r,f_n} is the amplitude of the force at excitation frequency f_n which can be obtained by using the FFT (Fast Fourier Transform) function, M is the mass of the motor, ω_m is the angular natural frequency of the mode m, and ω_n is the angular frequency of the force component of the order n.

In this model, only the circumferential modes of the stator is considered, the axial vibration is assumed as uniform. Based on the assumption, the acoustic wavenumber k_0 is determined

$$\sigma_{m} = \frac{(k_{0}R_{f})^{2} [Y_{m}(k_{0}R_{f})J_{m+1}(k_{0}R_{f}) - J_{m}(k_{0}a)Y_{m+1}(k_{0}R_{f})]}{[mJ_{m}(k_{0}R_{f}) - (k_{0}R_{f})J_{m+1}(k_{0}R_{f})]^{2} + [mY_{m}(k_{0}R_{f}) - (k_{0}R_{f})Y_{m+1}(k_{0}R_{f})]^{2}}$$
(15)

by the circumferencial direction wavenumber. Then the radiation efficiency of circumferencial mode can be expressed (15), where $J_m(k_0R_f)$ and $J_{m+1}(k_0R_f)$ are the first kind Bessel functions of the m^{th} and $(m+1)^{th}$ order respectively [31]. $Y_m(k_0R_f)$ and $Y_{m+1}(k_0R_f)$ and are the second kind of Bessel functions (Neumann functions) of the m^{th} and $(m+1)^{th}$ order, respectively. Next the sound power level can be calculated as;

$$SW(f_n) = 10\log_{10} \frac{\sum \Pi_m}{\Pi_{ref}}$$
 (16)

where the reference sound power $\Pi_{ref} = 10^{-12} W$. And the sound pressure level can be expressed as [33]

$$SPL_{f_n} = SW_{f_n} - 10\log_{10}\left\{2\pi\left[1 + \frac{\max(D_h, L_h)}{2}\right]^2\right\}$$
 (17)

V. VALIDATION OF THE MODEL

A. Experimental Set-up

An experimental set-up was developed for experimental validation. The parameters for the SRM under testing are listed in Table II. Fig. 8 presents the block digram of the experimatal setup. A three phases asymmetric bridge converter with 680V DC input was used to power the SRM motor. The phase current was controlled with hysteresis control.

TABLE II PARAMETERS OF 6/10 SRM

| Parameter | Value | Unit |
|-------------|-----------------------|------|
| Rated power | 3 HP | HP |
| Rated speed | 1800 RPM | RPM |
| Efficiency | >90% at rated speed | - |
| Housing | Outer diameter: 174.3 | mm |
| | Length: 183.5 | mm |

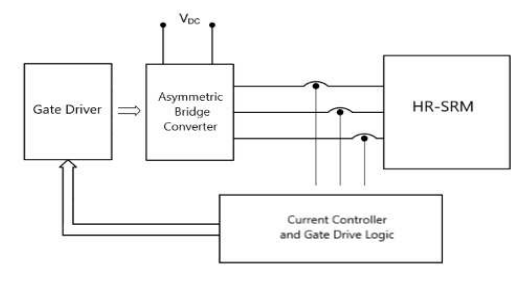


Fig. 8. Structure of the power converter of HR-SRM

The experimental set-up was built with a TMS320F28335 MCU from Texas Instruments, which has a maximum speed of 150 MIPS, and a 12-bit A/D converter built in. The sampling frequency was set at 20 kHz, which was enough for the hysteresis control. A 12 bit absolute encoder was used to provide shaft position feedback. Noise and vibration recordings are completed with Siemens LMS Test.lab. The microphone was placed 1 meter away form the motor in the perpendicular direction. The A-weighting was applied to the

sound pressure level measurement in an effort to account for the relative loudness perceived by the human ear. Fig. 9 shows photo of the experimental set-up.



Fig. 9. Experimental Set-Up of HR-SRM

A. Verification of Noise Estimations

The acoustic noise measurements were taken from the experimental setup to validate simulation results. Two arbitrary operating points are shown in this paper at 1500 RPM and 1800 RPM under 1Nm load. Figs. 10 and 11 show the acoustic noise level in term of sound pressure level in dB for both speeds at different resonance modes. Among the electromagnetic force components, the frequencies that are close to the natural frequencies of the stator are important to the stator vibration since the noise pressure level is approach to the maximum at those frequencies. It can be seen that FEA tends to estimate higher than experimental data, while analytical model gets closer results.

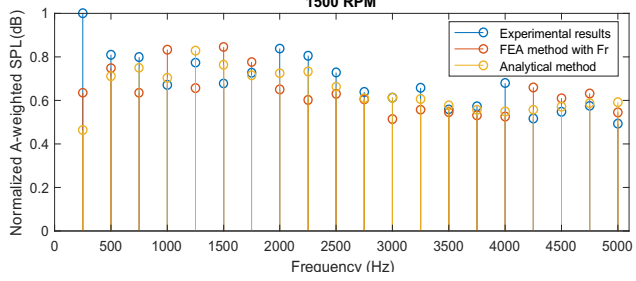


Fig. 10. Validation results at 1500 RPM with normalized values

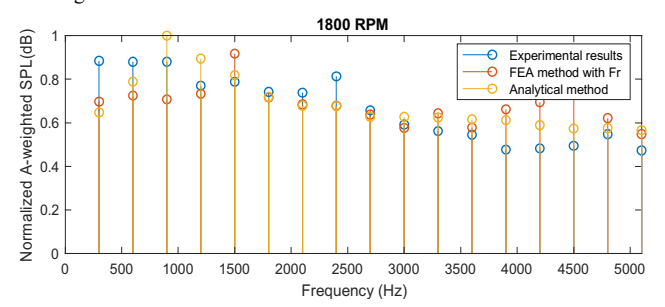


Fig. 11. Validation results at 1800 RPM with normalized values

In predicting the vibration and acoustic behaviours, performance of the hybrid model was impressive with faster esitimation speed and lower computational cost. FEA results show higher noise level estimations at some frequencies, which can be attributed to the fact that the 3D mechanics model was modeled as a rigid body. In experiments, the laminated structure motor has lower audible noise levels compared to

FEA results. The results of the hybrid model are comparable to the experimental data and they also require less setup time and computational effort than pure FEA models. The setup was developed on a modern computing platform with 28 CPU cores operating at 3.6 GHz clock speed and 128 GB Ram. Simulations for harmonics analysis of a complete 3D FEA model required approximately two hours to complete, and one additional hour for acoustic noise analysis.

VI. CONCLUSION AND FUTURE WORK

An analytical time-efficient model has been developed to predict noise and vibration in an SRM. Results obtained from the hybrid model have been compared to FEA and hardware measurements. The proposed model includes three main partsan electromagnetic model to calculate radial; a structural model to obtain resonance mode frequencies; and an NVH model to predict acoustic noise level. The developed model is very effective in estimating vibration modes and acoustic noise behaviour. The proposed hybrid model shows significantly lower simulation time, where the electromagnetic model saves nearly 30% of computational time compared to the FEA simulation. The acoustic model compared with FEA methods can reduce the computation time by nearly a factor of 30. The acoustic noise prediction model takes about 8 mins, while the FEA model needs over 2 hours for the current configuration. In summary, this hybrid approach can be an effective tool in minimizing the computational time for multi-objective and iterative optimization of excitation currents towards acoustic noise optimization.

ACKNOWLEDGMENT

This work was supported in part by the U.S. National Science Foundation under Grant 1927432 and by Turntide Technologies.

REFERENCE

- [1] Jin-Woo Ahn, Sung-Jun Park and Dong-Hee Lee, "Hybrid excitation of SRM for reduction of vibration and acoustic noise," in *IEEE Transactions on Industrial Electronics*, vol. 51, no. 2, pp. 374-380, April 2004.
- [2] S. Yaman, C. Chen, Z. Zhang and M. Krishnamurthy, "Acoustic Noise and Vibration in Switched Reluctance Machines: A Comparative Study of 12/8 and 8/6 Topologies," 2019 IEEE International Electric Machines & Drives Conference (IEMDC), San Diego, CA, USA, 2019, pp. 1130-1137.
- [3] R. D. Ciskowski and C. A. Brebbia, "Boundary element methods in acoustic," in *Computational Mechanics Elservier Applied Science*, Southampton, Boston, 1991.
- [4] Kirkup, Stephen, "The Boundary Element Method in Acoustics: A Development in Fortran," in *Integrated Sound Software*, 1998.
- [5] Henneberger, G., Sattler, P. K., & Shen, D. (1992). Nature of the equivalent magnetizing current for the force calculation. *IEEE Transactions on Magnetics*, 28(2), 1068–1071.
- [6] Coulomb, J. L. (1983). A methodology for the determination of global electromechanical quantities from a finite element analysis and its application to the evaluation of magnetic forces, torques and stiffness. *IEEE Transactions on Magnetics*, 19(6), 2514–2519.
- [7] Coulomb, J., & Meunier, G. (1984). Finite element implementation of virtual work principle for magnetic or electric force and torque computation. *Magnetics, IEEE Transactions* On, 20(5), 1894–1896.
- [8] L. H. de Medeiros, G. Reyne and G. Meunier, "About the distribution of forces in permanent magnets," in *IEEE Transactions on Magnetics*, vol. 35, no. 3, pp. 1215-1218, May 1999

- [9] Pile, R. (2018). Comparison of Main Magnetic Force Computation Methods for Noise and Vibration Assessment in Electrical Machines. *IEEE Transactions on Magnetics*, 54(7), 1–13.
- [10] F. Henrotte, G. Deliége, and K. Hameyer, "The eggshell approach for the computation of electromagnetic forces in 2D and 3D," COMPEL-Int. J. Comput. Math. Elect. Electron. Eng., vol. 23, no. 4, pp. 996–1005, 2004.
- [11] F. Henrotte, M. Felden, M. van der Giet, and K. Hameyer, "Electromagnetic force computation with the Eggshell method," in the 14th International Symposiumon Numerical Field Calculation in Electrical Engineering, IGTE 2010, Graz, Austria, 2010.
- [12] M. van der Giet, D. Franck, F. Henrotte, and K. Hameyer, "Comparative study of force computation methods for acoustic analyses of electrical machines," in *Proc. 14th IGTE Symp. Numer. Field Calculation Elect.* Eng., Graz, Austria, Sep. 2010, pp. 1–6.
- [13] S. Sathyan, A. Belahcen, U. Aydin, J. Kataja, V. Nieminen and J. Keränen, "Computational and experimental segregation of deformations due to magnetic forces and magnetostriction," 2017 20th International Conference on Electrical Machines and Systems (ICEMS), Sydney, NSW, 2017, pp. 1-6.
- [14] Karban, P., Korous, L., Mach, F., & Dolezel, I. (2014). Computation of forces in strongly nonlinear magnetic fields using higher-order eggshell algorithm.
- [15] Deliége, G & Henrotte, François & Vande Sande, Hans & Hameyer, K. (2003). 3D - finite element formulation for the computation of a linear transverse flux actuator. COMPEL: Int J for Computation and Maths. in Electrical and Electronic Eng. 22. 1077-1088.
- [16] Belytschko, B. and Hughes, T.J.R., Eds. 1983. Computational Methods for Transient Analysis, North Holland, Amsterdam.
- [17] Zeng, L.F., Wiberg, N.-E., and Bernspang, L., Adaptive finite element procedure for 2D dynamic transient analysis using direct integration, *Int. J. Numer. Methods Eng.*, 34, 997 – 1014, 1992.
- [18] Hughes, Thomas J. R. The Finite Element Method: Linear Static and Dynamic Finite Element Analysis. Prentice-Hall, Inc., Englewood Cliffs, New Jersey, 1987.
- [19] Cook, R.D., Malkus, D.S., and Plesha, M.E. 1989. Concepts and Applications of Finite Element Analysis, 3rd ed., Wiley, New York.
- [20] Shah VN, Bohm GJ, Nahavandi AN. Modal Superposition Method for Computationally Economical Nonlinear Structural Analysis. ASME. J. Pressure Vessel Technol. 1979;101(2):134-141.
- [21] N. F. Knight. "Nonlinear structural dynamic analysis using a modified modal method." AIAA Journal, vol. 23, 1985, pp. 1594-1601.
- [22] Wang, Erke, and Thomas Nelson. "Structural Dynamic Capabilities of ANSYS." Engineering Simulation & 3D Design Software, 23 Feb. 2017,
- [23] Hunt, John T., et al. "Finite Element Approach to Acoustic Radiation from Elastic Structures." The Journal of the Acoustical Society of America, vol. 55, no. 2, 1974, pp. 269–280.
- [24] Everstine, G.c. "Finite Element Formulatons of Structural Acoustics Problems." Computers & Structures, vol. 65, no. 3, 1997, pp. 307–321.
- [25] Kagawa, Y., Yamabuchi, T., Sugihara, K., & Shindou, T. (1980). A finite element approach to a coupled structural-acoustic radiation system with application to loudspeaker characteristic calculation. *Journal of Sound* and Vibration, 69(2), 229–243.
- [26] C. Lin, B. Fahimi, "Reduction of torque ripple in switched reluctance motor drives using field reconstruction method," *IEEE Vehicle Power* and Propulsion Conference (VPPC), 2011.
- [27] W. Zhu, B. Fahimi, "A field reconstruction method for optimal excitation of permanent magnet synchronous machines," *IEEE Trans. Energy Convers.*, vol. 21, no. 2, June 2006.
- [28] M. N. Anwar and O. Husain, "Radial force calculation and acoustic noise prediction in switched reluctance machines," in *IEEE Transactions on Industry Applications*, vol. 36, no. 6, pp. 1589-1597, Nov.-Dec. 2000.
- [29] S. J. Yang, Low-noise Electrical Motors, Clarendon press, 1981.
- [30] J. Ahn, S. Oh, J. Moon and Y. Hwang, "A three-phase switched reluctance motor with two-phase excitation," *IEEE Trans. on Ind. Appl.*, vol. 35, no. 5, pp. 1067-1075, Sept.-Oct. 1999
- [31] P. L. Timar, A. Fazekas, J. Kiss, A. Miklos and S.J. Yang, Noise and Vibration of Electrical Machines, Elsevier, Amsterdam – Oxford – New York – Tokyo, Japan, 1989.
- [32] J. F. Gieras, C. Wang, J. C. Lai, *Noise of Polyphase Electric Motors*, Taylor & Francis Group, CRC Press, 2006.
- [33] J. W. Jiang, J. Liang, J. Dong, B. Howey, and A. D. Callegaro, Switched Reluctance Motor Drives: Fundamentals to Applications, vol. 1. Boca Raton, FL, USA: CRC Press, 2018.